JOURNAL OF CHEMICAL & ENGINEERING DATA

ARTICLE

pubs.acs.org/jced

CO_2 Capture Capacity and Swelling Measurements of Liquid-like Nanoparticle Organic Hybrid Materials via Attenuated Total Reflectance Fourier Transform Infrared Spectroscopy

Youngjune Park,[†] Dolly Shin,[†] Young Nam Jang,[‡] and Ah-Hyung Alissa Park*[,†]

[†]Department of Earth and Environmental Engineering, Department of Chemical Engineering, and Lenfest Center for Sustainable Energy, Columbia University, New York, New York 10027, United States

[‡]Korea Institute of Geoscience and Mineral Resources, 30 Gajeong-dong, Youseung-gu, Daejeon, Republic of Korea

ABSTRACT: Novel nanoparticle organic hybrid materials (NOHMs), which are comprised of organic oligomers or polymers tethered to an inorganic nanosized cores of various sizes, have been synthesized, and their solvating property for CO_2 was investigated using attenuated total reflectance (ATR) Fourier transform infrared (FT-IR) spectroscopy. Simultaneous measurements of CO_2 capture capacity and swelling behaviors of polyetheramine (Jeffamine M-2070) and its corresponding NOHMs (NOHM-I-PE2070) were reported at temperatures of (298, 308, 323 and 353) K and CO_2 pressure conditions ranging from (0 to 5.5) MPa. The polymeric canopy, or polymer bound to the nanoparticle surface, showed significantly less swelling behavior with enhanced or comparable CO_2 capture capacity compared to pure unbound polyetheramine.

INTRODUCTION

With the increasing attention to climate debate, the removal of CO_2 from a flue-gas stream generated from coal-fired power plants or other large point sources of anthropogenic CO_2 has become an urgent issue. Until now, aqueous solutions of amines or ammonia have been considered for the postcombustion capture of CO_2.[1,2] These conventional solvents exhibit great CO_2 capture capacities, while their inherent properties often provoke the following undesired effects during CO_2 capture: (i) the corrosion of the reactor or plant structures, (ii) the loss of the solvent due to vaporization or degradation, and (iii) the high parasitic energy consumption during the solvent regeneration process due to the high water content (70 to 85 wt %).[3,4] Thus, the development of alternative materials, which possess high CO_2 capture capacity, greater oxidative and thermal stability, lower vapor pressure, and lower energy requirements for regeneration, has become necessary.

Recently, organic−inorganic hybrid materials based on the nanoparticles, called nanoparticle organic hybrid materials (NOHMs), have been developed.[5] NOHMs consist of inorganic nanosized cores and ionically or covalently tethered organic canopy species (Figure 1). NOHMs can be synthesized in various forms ranging from glassy solids to solvent-free nanoparticle ionic fluids. Because the polymeric canopy species could act as a fluid medium, it allows NOHMs to exhibit liquid-like behaviors without the agglomeration of the nanoparticles. Unique characteristics of NOHMs such as tuned optical, electrical, and thermal properties have been reported.[5−8] Therefore, NOHMs are expected to be applicable for a wide variety of technologies in addition to CO_2 capture, including photovoltaics, water desalination, and oil exploration.[6−11]

To investigate the potential of NOHMs as a CO_2 capture medium, this study focused on the CO_2 solvating ability of NOHMs based on the following unique structural properties of NOHMs: (i) The organic species strongly bound to hard spheres of nanoparticles can reduce the inherent vapor pressure of organic materials and elevate the operating temperature by increasing thermal stability. (ii) The organic canopy species are densely grafted onto nanoparticles, and they fill the gap between nanoparticles; thus, the frustration or spontaneous ordering of canopy chains could occur due to steric and/or entropic effects. This could result in small gaseous molecules such as CO_2 being accommodated favorably by reducing the free energy of the frustrated canopy. (iii) The addition of task-specific functional groups such as amines can provide sites for chemical interactions between the organic canopy and CO_2 molecules, while the ordered structure of the canopy chains may provide greater accessibility to those functional sites. Thus, NOHMs could exhibit promising CO_2 capture capacity and selectivity. Recently, Lin and Park reported that NOHMs exhibited relatively good selectivity for CO_2 against N_2 and O_2.[12] For the optimization of NOHMs as a CO_2 capture medium, both entropic and enthalpic effects of NOHMs should be tuned. In this study, the CO_2 capture capacity and swelling behaviors of the synthesized NOHMs without task-specific functional groups were investigated to isolate the entropic effect, and the results were compared with those of pure canopy material.

EXPERIMENTAL SECTION

For the synthesis of NOHMs, colloidal suspensions of silica with diameters of (7, 12, and 22) nm (Ludox colloidal silica, Sigma Aldrich (Milwaukee, WI)) were used. The diluted solution of silica nanoparticles (3 wt %) was added to 3-(trihydroxysilyl)-1-propane sulfonic acid (6 wt %, Gelest Inc. (Morrisville, PA)),

Received: June 22, 2011
Accepted: October 12, 2011
Published: October 28, 2011

ACS Publications © 2011 American Chemical Society

and then sodium hydroxide (1 M) was added to adjust the pH to 5. The suspension mixture was incubated at 343 K for 12 h with constant stirring. The excess silane was removed in the dialysis tubing (3.5k MWCO, Pierce Biotechnology Inc. (Rockford, IL)) for 48 h. To attach polymeric canopy to the surface of the nanoparticles, a cation exchange column (Dowex HCR-W2, Dow Chemical Co.) was used to replace sodium ions with protons. Jeffamine M-2070 (polyetheramine, $M_w \sim 2000$, Huntsman Co. (The Woodlands, TX)) was selected as the canopy material. The diluted solution of Jeffamine M-2070 (10 wt %) was added to the functionalized nanoparticle suspension, and the final product was dried under vacuum at 308 K for at least 36 h to remove the excess water. Finally NOHMs (denoted as NOHM-I-PE2070 where I and PE2070 represent the "ionically" tethered canopy and "Jeffamine M-2070", respectively) with different core sizes were obtained.[12] The weight percent of inorganic cores in NOHM-I-PE2070 was measured by using a thermogravimetric analyzer (Q50, TA Instruments Inc. (New Castle, DE)) and found to be ~15 wt % for all prepared NOHMs samples.

A Fourier-transform infrared (FT-IR) spectrometer (Nicolet 6700, Thermo Fisher Scientific Inc. (Madison, WI)) equipped with a deuterated triglycine sulfate (DTGS) detector was used to measure the CO_2 capture capacity and swelling behaviors of NOHM-I-PE2070. All spectra were obtained from the acquisition of 32 scans, the resolution of 2 cm^{-1}, and the spectrum range of 4000 cm^{-1} to 525 cm^{-1}. The interferograms were multiplied by the Norton−Beer "medium" apodization function prior to the Fourier transformation. To measure the CO_2 capture capacity and swelling behavior simultaneously, an attenuated total reflectance (ATR) accessory with high-pressure cell (Golden Gate Supercritical Fluids analyzer, Specac Inc. (Cranston, RI)) was installed to the FT-IR. The incident angle of the infrared beam was 43° (± 1°) and it was focused with zinc selenide (ZnSe) lenses. In the ATR apparatus, a thin layer of NOHM-I-PE2070 samples was applied to the top of the diamond crystal which is mounted on the heating plate connected with a PID temperature controller. Each sample was measured at temperatures of (298, 308, 323 and 353) K. To apply the desired CO_2 pressure of (0 to 55) MPa, a pressure generator (High Pressure Generators, HiP Co. (Erie, PA)) was employed. All NOHM-I-PE2070 samples were in the liquid or liquid-like states above room temperature, which offered a good contact with the diamond crystal. Each equilibrium was attained by observing the change in absorbance, and the typical time spent to reach the equilibrium was less than 10 min. The experimental apparatus is shown in Figure 2.

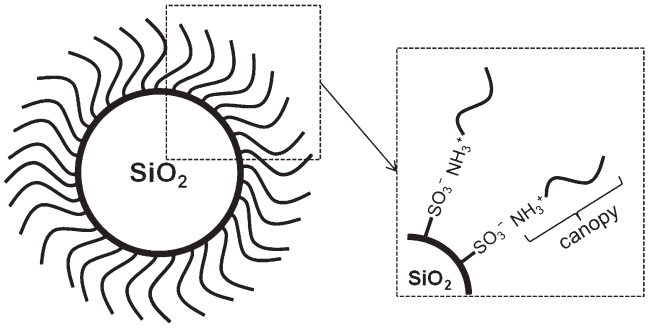

Figure 1. Schematic diagram of ionically tethered NOHMs with a polymeric canopy.

RESULTS AND DISCUSSION

It is known that a chemical affinity toward CO_2 and/or accessibility of CO_2 to functional groups in polymeric materials can significantly affect the CO_2 capture behavior.[13] Because NOHMs consist of organic canopy species tethered to inorganic nanoparticles, they can offer an organic−inorganic hybrid matrix to tune both chemical affinity and accessibility for CO_2 via specific intermolecular interactions and unique structural arrangements of canopy species. Therefore, the simultaneous investigation of swelling behaviors of NOHMs during CO_2 loading could provide important information about the structural behavior of NOHMs and the extent of the entropy effect on the solvating ability of NOHMs as well as more rigorous interpretation of sorption process.

The techniques previously used for the measurement of both CO_2 sorption and swelling behavior of polymeric materials include in situ spectroscopy measurements with visual observation and gravimetric experiments with barometric methods.[14−16] In this study, a FT-IR spectrometer coupled with a high pressure

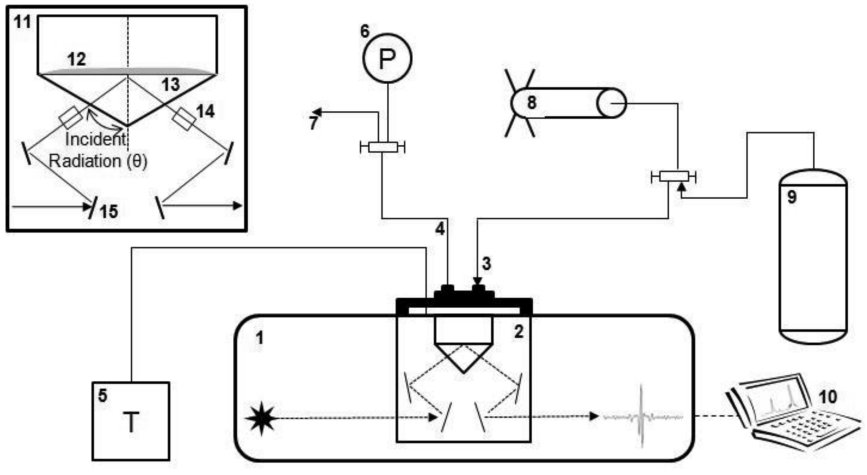

Figure 2. Schematic diagram of in situ CO_2 capture capacity and swelling measurements apparatus. (1) FT-IR spectrometer, (2) ATR optics and high pressure fluid cell, (3) gas inlet, (4) gas outlet, (5) PID temperature controller, (6) pressure gauge, (7) vent, (8) pressure generator, (9) CO_2 reservoir, (10) data processing computer, (11) enlarged view of ATR cell, (12) sample, (13) diamond crystal, (14) ZnSe lenses, (15) mirrors.

dx.doi.org/10.1021/je200623b |J. Chem. Eng. Data 2012, 57, 40–45

ATR technique was used to investigate the CO_2 capture capacity and swelling behaviors of NOHM-I-PE2070, simultaneously. The ATR FT-IR approach has been developed by Flichy et al. for the simultaneous measurements of swelling and CO_2 sorption for pure polymers.[17] ATR FT-IR spectroscopy is one of the most promising tools for investigating the thermodynamic and kinetic properties during the CO_2 sorption in polymeric matrix in particularly in high-pressure and high-temperature conditions, while observing the specific intermolecular interactions between each functional group.[18] The inherent nature of ATR often provokes peak distortions and/or less accuracy in quantitative analysis for the CO_2 sorption system compared to barometric or gravimetric approaches.[19,20] This is due to several assumptions and uncertainty in calculations. However, ATR can provide an insight to the understanding of the CO_2 sorption mechanisms in polymeric matrix with regards to its structural behavior such as swelling.

Generally, infrared transparent materials such as ZnSe, germanium, silicon, zinc sulfur, KRS-5 (thallium iodide and chloride), and diamond are used as internal reflection elements for ATR FT-IR spectroscopy. The internally reflected infrared radiation at the interface between the transparent crystal material and the sample specimen creates an evanescent electric field, and its intensity undergoes an exponential decay as given in the following equation,

$$E = E_0 \cdot e^{-z/d_p} \tag{1}$$

where E is the electric field amplitude at a penetration distance into the sample z, E_0 is the electric field amplitude at the interface, and d_p is the penetration depth given by

$$d_p = \frac{\lambda}{2\pi(n_1^2 \sin^2\theta - n_2^2)^{1/2}} \tag{2}$$

where λ is the wavelength of the incident beam, θ is the incident angle, and n_1 and n_2 are the refractive indices of the ATR crystal and the sample, respectively. To quantify the CO_2 capture capacity from the ATR FT-IR spectra, the volume of the evanescent wave, also known as the effective path length (d_e), should be given. The effective path length of the evanescent wave in an ATR measurement can be defined as the equivalent path in a transmission measurement, developed by Harrick.[21] In this approach, the Beer−Lambert law is modified by replacing d with d_e. The modified Beer−Lambert law which expresses the relationship among the absorbance (A), absorptivity (ε), concentration (c), and infrared path length (d_e), is written as,

$$A = \varepsilon \cdot c \cdot d_e \tag{3}$$

where the d_e is the arithmetical mean between the effective path length for the perpendicular ($d_{e\perp}$) and the parallel ($d_{e\parallel}$) polarization. The effective path lengths of the polarization are defined as

$$d_{e\perp} = \frac{n_1^2 n_2 \cos\theta}{(n_1^2 - n_2^2)} \cdot \frac{\lambda}{\pi\sqrt{n_1^2 \sin^2\theta - n_2^2}} \tag{4}$$

$$d_{e\parallel} = \frac{n_1^2 n_2 \cos\theta}{(n_1^2 - n_2^2)} \cdot \frac{2n_1^2 \sin^2\theta - n_2^2}{(n_1^2 - n_2^2)\sin^2\theta - n_2^2} \cdot \frac{\lambda}{\pi\sqrt{n_1^2 \sin^2\theta - n_2^2}} \tag{5}$$

For the calculation of the CO_2 capture capacity in NOHM-I-PE2070 samples, required input data were the refractive index of ATR crystal (diamond) = 2.42, the angle of the incidence = 43°, and the wavelength of asymmetric stretching band of CO_2 (ν_3) = 2336 cm^{-1}. The absorbance of CO_2 was quantified by measuring the intensity of ν_3 band, while assuming its molar absorptivity at high pressure to be $1.0 \cdot 10^6$ $cm^2 \cdot mol^{-1}$.[22] The molar absorptivity of CO_2 in the ν_3 band used in this study is for the high-pressure condition, and thus it gives relatively accurate values of CO_2 capture capacity under high-pressure; however, its accuracy may not be as high in low-pressure measurements.[17,23] The refractive index of NOHM-I-PE2070 (n_D = 1.52) was measured by using an ellipsometer (α-SE, J.A. Woollam Co., Inc. (Lincoln, NE)). Finally, the obtained concentrations of CO_2 were used to calculate the CO_2 capture capacity in NOHM-I-PE2070 using eq 3. To facilitate the comparison between the organic portion of NOHM-I-PE2070 and its corresponding pure polymer (Jeffamine M-2070), the concentration of CO_2 absorbed in NOHM-I-PE2070, c, was calculated excluding nanoparticle by using the following equation[17]

$$m_{CO_2}(\text{mmol} \cdot g^{-1}) = \frac{c_{CO_2}(g \cdot cm^{-3})}{\frac{\rho}{(1 + S)}} \tag{6}$$

where ρ is the density and S is the degree of swelling of NOHM-I-PE2070. The degree of swelling of NOHM-I-PE2070 is defined by

$$S = \frac{A^0}{A} \cdot \frac{d_e}{d_e^0} - 1 \tag{7}$$

where A^0, d_e^0, A, and d_e are the absorbance and the effective path lengths without and with CO_2, respectively. Both absorbances of C−O (~1100 cm^{-1}) and C−H (~2865 cm^{-1}) bands were selected for the swelling measurements. Because the broad band of Si−O stretching of the nanoparticle cores (~1057 cm^{-1}) overlaps with C−O band of canopy chains, the swelling ratios obtained via the integration in the interval from 1200 cm^{-1} to 1000 cm^{-1} would more likely represent the volume change of entire NOHM system including both inorganic and organic parts. On the other hand, the integration of the absorbance in the interval from 3000 cm^{-1} to 2700 cm^{-1} was performed to represent the swelling behavior of the polymeric canopy in NOHMs. It was assumed that the absorptivity was not significantly affected by the concentration of CO_2 at different pressures, and thus, the change in the effective thickness was considered to be negligible.[17,23−25]

Figure 3 shows the ATR FT-IR spectra of NOHM-I-PE2070 before and after CO_2 loading. As CO_2 was absorbed into the polymeric canopy of NOHMs, significant intensity changes were observed for each absorption band. Due to the volume change during CO_2 absorption, the two characteristic peaks of CO_2 in the mid-IR region, asymmetric stretching (ν_3, at 2335 cm^{-1}) and bending mode (ν_2, ~659 cm^{-1}), were increased, while other absorption bands from the canopy were decreased.

The ATR FT-IR spectra were obtained for temperatures of (298, 308, 323, and 353) K and the CO_2 pressure range of (0 to 5.5) MPa, and CO_2 capture capacities of NOHM-I-PE2070 with varying sizes of nanoparticles were calculated. Figure 4 presents CO_2 capture capacities of unbound Jeffamine M-2070 and bound Jeffamine M-2070 in NOHMs as a function of CO_2 pressure under various temperature conditions. It was observed that the CO_2 capture capacity of the polymeric canopy attached to the nanoparticles increased with increasing CO_2 pressure for each isotherm, and as temperature increased the CO_2 capture capacity decreased. In all cases, the organic canopy of NOHM-I-PE2070

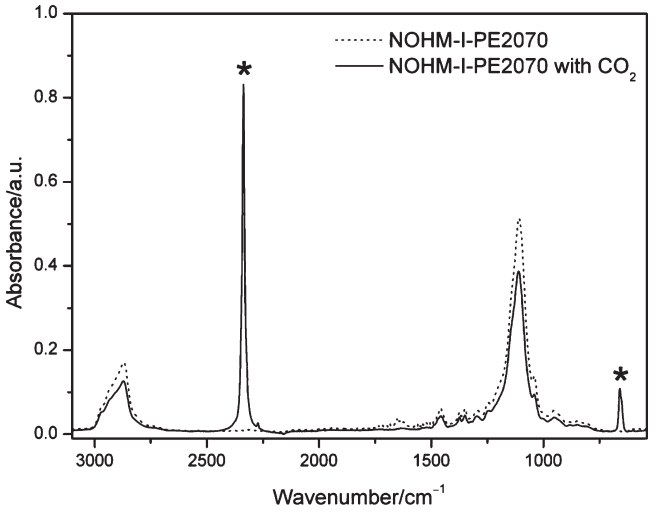

Figure 3. ATR FT-IR spectra of NOHM-I-PE2070 before and after exposure to CO_2 at 5.5 MPa and 298 K. CO_2 absorption bands are marked with asterisks.

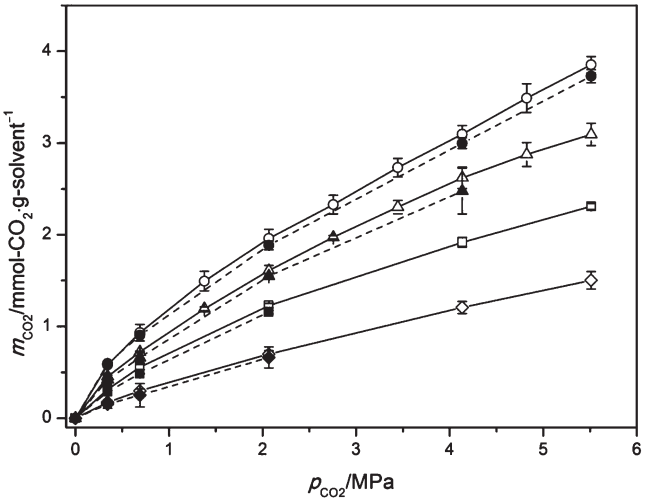

Figure 4. CO_2 capture capacities of pure polymer (Jeffamine M-2070, solid symbols) and its corresponding NOHMs (NOHM-I-PE2070 with 7 nm diameter SiO_2 core, open symbols) as a function of p_{CO_2} under various temperature conditions (●, ○, ~298 K; ▲, △, ~308 K; ■, □, ~323 K; ♦, ◊, ~353 K).

consistently achieved slightly higher or comparable CO_2 capture capacities compared to the unbound polymer. Although NOHM-I-PE2070 investigated in this study were designed without task-specific functional groups such as amines, it was observed that ether groups in the polymeric canopy interacted with CO_2 through Lewis acid−base interactions.[26] Therefore, the combined effect of the structural change due to the entropic effect (i.e., ordering or arrangement of the canopy chains) and the Lewis acid−base interaction possibly resulted in enhanced CO_2 capture capacity in NOHM-I-PE2070. As shown in Figure 4, the degree of the enhancement in CO_2 capture using NOHMs over pure polymer was not very significant but definitely consistent. Moreover, it is important to point out that pure polymer has much lower thermal stability than the canopy tethered to nanoparticles.[12] The enhancement in NOHMs' thermal stability

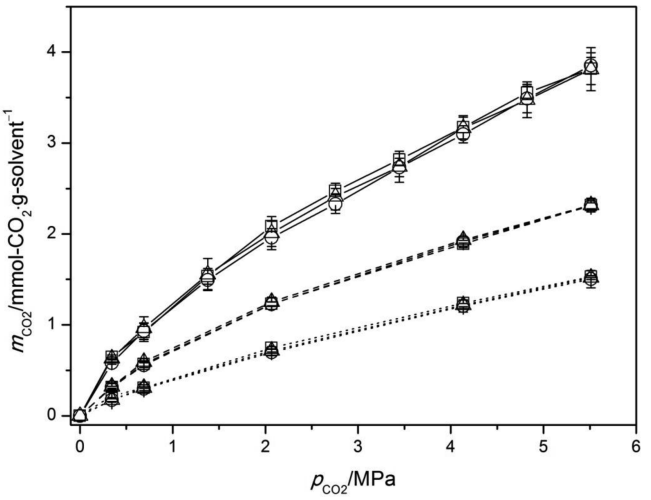

Figure 5. CO_2 capture capacities of NOHM-I-PE2070 with different SiO_2 core sizes (○, 7 nm diameter; △, 12 nm diameter; □, 22 nm diameter) at temperatures of 298 K (solid lines), 323 K (dashed lines), and 353 K (dotted lines).

along with their improved CO_2 capture capacity concludes that NOHMs could have potential benefits as CO_2 capture medium compared to pure polymers.

The CO_2 capture capacity was also measured with varying sizes of nanoparticles (Figure 5); however, no clear relationship between the CO_2 capture capacity and the nanoparticle size was observed among the prepared NOHM-I-PE2070 samples. It is supposed that a ratio of core diameter (d) and canopy's radius of gyration (R_g) could be an important structural variable which may alter the intercanopy interactions or solvating properties for CO_2. The details of these capture mechanisms covering a larger R_g/d value with varying grafting density and steric hindrance will be subject to future investigations.

Because CO_2 absorption would induce a volume change in polymeric material and result in swelling, the investigation of the swelling behavior of NOHMs could provide insight into their CO_2 capture mechanisms. The degree of swelling of NOHM-I-PE2070 was measured at 298 K with varying sizes of nanoparticles (Table 1). Similar to the case of CO_2 capture capacity, the size of nanoparticles did not significantly affect the degree of swelling during CO_2 capture. Figure 6 shows the relationship between the CO_2 capture capacities and the swelling (%) of the polymeric canopy of NOHM-I-PE2070, and the results were compared with that of Jeffamine M-2070. NOHM-I-PE2070 distinctly showed a different swelling pattern from Jeffamine M-2070. For the same amount of CO_2 capture, the swelling (%) of NOHM-I-PE2070 was significantly less than that of the unbound polymer system. It is speculated that the frustrated canopy chains in NOHMs would favor the incorporation of CO_2 between them, and therefore, NOHMs would require less swelling to absorb the same amount of CO_2.

The maximum wavenumbers of the absorbance of C−O stretching bands of both unbound Jeffamine M-2070 and bound canopy showed blue shifts as more CO_2 was absorbed. Figure 7 presents the patterns of the peak shift of the C−O stretching band as a function of p_{CO_2}. Generally this type of increase in wavenumber occurs when the interaction between the polymeric chains and the surrounding environment decreases.[17,27] In this study, this seems to have happened because, as more CO_2 was

Table 1. Swelling Behaviors of the Polymeric Canopy in NOHM-I-PE2070 with Various SiO_2 Core Sizes and Jeffamine M-2070 at T/K = 298

NOHM-I-PE2070 (7 nm)		NOHM-I-PE2070 (12 nm)		NOHM-I-PE2070 (22 nm)		Jeffamine M-2070	
p_{CO_2}/MPa	S/%	p_{CO_2}/MPa	S/%	p_{CO_2}/MPa	S/%	p_{CO_2}/MPa	S/%
0.3	3.56 (± 0.4)	0.3	2.94 (± 0.1)	0.3	3.12 (± 0.1)	0.3	3.50 (± 0.1)
0.7	5.78 (± 0.42)	0.7	4.79 (± 0.53)	0.7	4.72 (± 0.5)	0.7	5.41 (± 0.8)
1.4	9.68 (± 0.42)	1.4	9.09 (± 0.79)	1.4	9.3 (± 0.47)	2.1	15.35 (± 1.35)
2.1	14.16 (± 0.44)	2.1	13.35 (± 0.66)	2.1	13.02 (± 0.71)	4.1	36.11 (± 1.7)
2.8	19.08 (± 0.61)	2.8	18.66 (± 1.2)	2.8	18.27 (± 0.72)	5.5	55.14 (± 2.7)
3.4	24.55 (± 0.05)	3.4	24.24 (± 1.43)	3.4	23.88 (± 0.2)		
4.1	30.82 (± 0.91)	4.1	30.29 (± 1.51)	4.1	29.86 (± 1)		
4.8	38.01 (± 0.78)	4.8	37.87 (± 1.52)	4.8	36.66 (± 1.49)		
5.5	46.8 (± 0.128)	5.5	45.97 (± 2.82)	5.5	45.19 (± 1.5)		

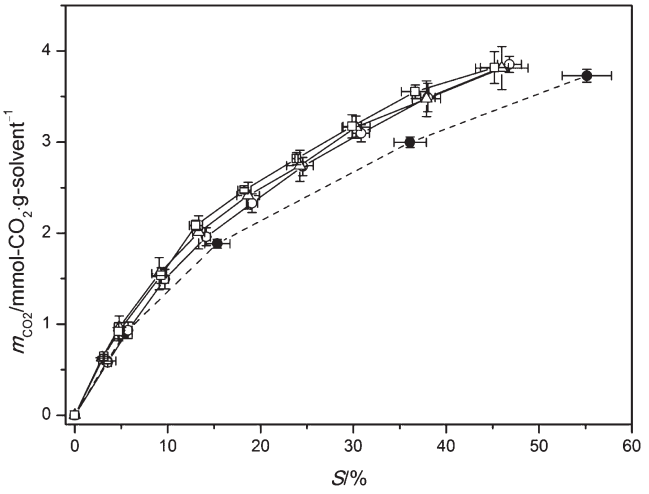

Figure 6. CO_2 capture capacities of pure polymer (Jeffamine M-2070, ●) and its corresponding NOHMs (NOHM-I-PE2070 with various SiO_2 core sizes) versus the volume increases at 298 K (○, 7 nm diameter; △, 12 nm diameter; □, 22 nm diameter).

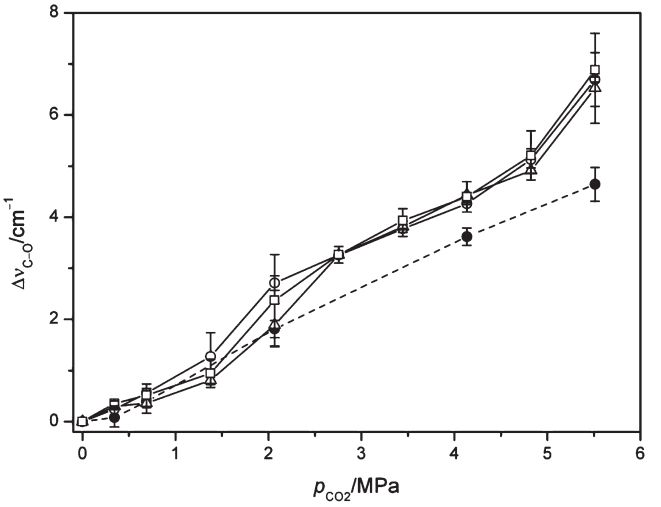

Figure 7. Spectral peak shifts of C−O stretching band of pure polymer (Jeffamine M-2070, ●) and its corresponding NOHMs (NOHM-I-PE2070 with various SiO_2 core sizes) as a function of p_{CO_2} at 298 K (○, 7 nm diameter; △, 12 nm diameter; □, 22 nm diameter).

absorbed, the mobility of each segment of canopy chain was increased. However, the polymeric canopy of NOHMs exhibited different shifting patterns compared to pure unbound polymer. Interestingly, the degree of peak shifts of NOHN-I-PE2070s C−O stretching band increased abruptly at (2 and 5) MPa CO_2 pressures, whereas that of pure polymer exhibited a monotonic increase over the same CO_2 pressure range. The peak shifts were relatively small in each step and uncertainty could exist in the patterns. However, the consistency in the peak shift patterns suggests that the frustrated canopies filled the gaps between core nanoparticles and the structural changes in the NOHMs' canopy compared to pure polymers allowed for improved accessibility of CO_2 to the functional sites in the NOHMs' canopy. The swelling behavior given in Figure 6 also supports this hypothesis. Future studies are needed to fully understand this interesting CO_2 capture mechanisms in detail.

CONCLUSIONS

In this study, the CO_2 capture capacities and swelling behaviors of NOHMs (i.e., NOHM-I-PE2070) were investigated at temperatures of (298, 308, 323, and 353) K and CO_2 pressures ranging from (0 to 5.5) MPa. The polymeric canopy material of NOHM-I-PE2070 showed distinct swelling behavior with enhanced or comparable CO_2 capture capacity compared to that of the pure polymer, Jeffamine M-2070. Based on the findings from this study the NOHMs will be further optimized for effective CO_2 capture.

AUTHOR INFORMATION

Corresponding Author

*Tel.: 212-854-8989. Fax: 212-854-7081. E-mail: ap2622@columbia.edu.

Funding Sources

This publication was based on work supported in part by Award No. KUS-C1-018-02, made by King Abdullah University of Science and Technology (KAUST), and the Utilization and Sequestration of CO_2 using Industrial Minerals Program by Korea Institute of Geoscience & Mineral Resources (KIGAM).

REFERENCES

(1) Astarita, G. Carbon dioxide absorption in aqueous monoethanolamine solutions. *Chem. Eng. Sci.* **1961**, *16*, 202–207.

(2) Rochelle, G. T. Amine scrubbing for CO_2 capture. *Science* **2009**, *325*, 1652–1654.
(3) Huang, H. Y.; Chinn, D.; Munson, C. L.; Yang, R. T. Amine-grafted MCM-48 and silica xerogel as superior sorbents for acidic gas removal from natural gas. *Ind. Eng. Chem. Res.* **2003**, *42*, 2427–2433.
(4) Aron, D.; Tsouris, C. Separation of CO_2 from flue gas: a review. *Sep. Sci. Technol.* **2005**, *40*, 321–348.
(5) Rodriguez, R.; Herrera, R.; Archer, L. A.; Giannelis, E. P. Nanoscale ionic materials. *Adv. Mater.* **2008**, *20*, 4353–4358.
(6) Bourlinos, A. B.; Herrera, R.; Chalkias, N.; Jiang, D. D.; Zhang, Q.; Archer, L. A.; Giannelis, E. P. Surface-functionalized nanoparticles with liquid-like behavior. *Adv. Mater.* **2005**, *17*, 234–237.
(7) Agarwal, P.; Qi, H.; Archer, L. A. The ages in a self-suspended nanoparticle liquid. *Nano Lett.* **2010**, *10*, 111–115.
(8) Nugent, J. L.; Moganty, S. S.; Archer, L. A. Nanoscale organic hybrid electrolytes. *Adv. Mater.* **2010**, *22*, 3677–3680.
(9) Bourlinos, A. B.; Chowdhury, S. R.; Herrera, R.; Jiang, D. D.; Zhang, Q.; Archer, L. A.; Giannelis, E. P. Functionalized nanostructures with liquid-like behavior: expanding the gallery of available nanostructures. *Adv. Funct. Mater.* **2005**, *15*, 1285–1290.
(10) Bourlinos, A. B.; Giannelis, E. P.; Zhang, Q.; Archer, L. A.; Floudas, G. Surface-functionalized nanoparticles with liquid-like behavior: the role of the constituent components. *Eur. Phys. J. E* **2006**, *20*, 109–117.
(11) Bourlinos, A. B.; Stassinopoulos, A.; Anglos, D.; Herrera, R.; Anastasiadis, S. H.; Petridis, D.; Giannelis, E. P. Functionalized ZnO nanoparticles with liquidlike behavior and their photoluminescence properties. *Small* **2006**, *2*, 513–516.
(12) Lin, K.-Y. A.; Park, A.-H. A. Effects of bonding types and functional groups on CO_2 capture using novel multiphase systems of liquid-like nanoparticle organic hybrid materials. *Environ. Sci. Technol.* **2011**, *45*, 6633–6639.
(13) Kemmere, M. F.; Meyer, T. *Supercritical carbon dioxide in polymer reaction engineering*; Wiley-VCH Verlag Gmbh & Co. KGaA: Weinheim, Germany, 2005.
(14) Wissinger, R. G.; Paulaitis, M. E. Swelling and sorption in polymer−CO_2 mixtures at elevated pressures. *J. Polym. Sci., Part B: Polym. Phys.* **1987**, *25*, 2497–2510.
(15) Vincent, M. F.; Kazarian, S. G.; West, B. L.; Berkner, J. A.; Bright, F. V.; Liotta, C. L.; Eckert, C. A. Cosolvent effects of modified supercritical carbon dioxide on cross-linked poly(dimethylsiloxane). *J. Phys. Chem. B* **1998**, *102*, 2176–2186.
(16) Hilic, S.; Padua, A. A. H.; Grolier, J. P. E. Simultaneous measurement of the solubility of gases in polymers and of the associated volume change. *Rev. Sci. Instrum.* **2000**, *71*, 4236–4241.
(17) Flichy, N. M. B.; Kazarian, S. G.; Lawrence, C. J.; Briscoe, B. J. An ATR-IR study of poly(dimethylsiloxane) under high pressure carbon dioxide: simultaneous measurement of sorption and swelling. *J. Phys. Chem. B* **2002**, *106*, 754–759.
(18) Stuart, B. *Infrared spectroscopy fundamentals and applications*; Wiley: Chichester, 2004.
(19) Averett, L. A.; Griffiths, P. R. Effective path length in attenuated total reflection spectroscopy. *Anal. Chem.* **2008**, *80*, 3045–3049.
(20) Duarte, A. R.; Anderson, L. E.; Duarte, C. M. M.; Kazarian, S. G. A comparison between gravimetric and in situ spectroscopic methods to measure the sorption of CO_2 in a biocompatible polymer. *J. Supercrit. Fluids* **2005**, *36*, 160–165.
(21) Harrick, N. J. *Internal reflection spectroscopy*; Interscience Publishers: New York, 1967.
(22) Maiella, P. G.; Schoppelrei, J. W.; Brill, T. B. Spectroscopy of hydrothermal reactions. part XI: infrared absorptivity of CO_2 and N_2O in water at elevated temperature and pressure. *Appl. Spectrosc.* **1999**, *53*, 351–355.
(23) Pasquali, I.; Andanson, J.-M.; Kazarian, S. G.; Bettini, R. Measurement of CO_2 sorption and PEG 1500 swelling by ATR-IR spectroscopy. *J. Supercrit. Fluids* **2008**, *45*, 384–390.
(24) Goodman, A. L. A comparison study of carbon dioxide adsorption on polydimethylsiloxane, silica gel, and Illinois no. 6 coal using in situ infrared spectroscopy. *Energy Fuels* **2009**, *23*, 1101–1106.
(25) Baschetti, M. G.; Piccinini, E.; Barbari, T. A.; Sarti, G. C. Quantitative analysis of polymer dilation sorption using FTIR-ATR spectroscopy. *Macromolecules* **2003**, *36*, 9574–9584.
(26) Nalawade, S. P.; Picchioni, F.; Marsman, J. H.; Janssen, L. P. B. M. Supercritical carbon dioxide ($scCO_2$) induced gelatinization of potato starch. *J. Supercrit. Fluids* **2006**, *36*, 236–244.
(27) Andanson, J.-M.; Jutz, F.; Baiker, A. J. Supercritical CO_2/ionic liquid systems: what can we extract from infrared and Raman spectra? *J. Phys. Chem. B* **2009**, *113*, 10249–10254.